

Optical properties of monolayer lattice and three-dimensional photonic crystals using dielectric spheres

S. Yano* and Y. Segawa

Photodynamics Research Center, The Institute of Physical and Chemical Research (RIKEN), Sendai 980-0845, Japan

J. S. Bae and K. Mizuno

Research Institute of Electrical Communication, Tohoku University, Sendai 980-8577, Japan

S. Yamaguchi and K. Ohtaka

Department of Applied Physics, Faculty of Engineering, Chiba University, Chiba 263-0022, Japan

(Received 14 March 2002; published 26 August 2002)

The transmittance spectra for the monolayer triangle lattice using millimeter-sized Si_3N_4 spheres are measured and calculated at various incident angles of electromagnetic waves. From the results, the dispersion of photonic bands for the monolayer triangle lattice is obtained. Furthermore, the transmittance spectra of three-dimensional layered photonic crystals are measured for different layer numbers and different air gaps. Theoretical analysis shows that the photonic band gaps refer to the anticrossing between heavy photon bands and light photon bands. Finally, we discuss the future prospect of the photonic crystals using dielectric spheres.

DOI: 10.1103/PhysRevB.66.075119

PACS number(s): 42.70.Qs

I. INTRODUCTION

There has been large interest in photonic crystals consisting of spatially periodic dielectric structures to bring about band structures for photons,^{1–3} whereas the full three-dimensional (3D) photonic crystal exhibits much more profound effects such as much stronger confinement effect and stop-band characteristics over a broader range of angles or even in all directions of light similar to the electronic band gaps in semiconductors.

The properties of photonic crystals based on dielectric spheres have been studied theoretically^{4–12} and experimentally.^{13–23} The important advantage of the arrayed spheres is that the behavior of the light (electromagnetic wave) in these photonic crystals is understood by the analogy of an electron in solid-state crystals, because the dielectric spheres are regarded as “optical” atoms. In this concept, the photonic crystals based on the arrayed dielectric spheres are fundamental systems to understand their optical properties.

Recently, we have studied the photonic band effect of a 2D monolayer lattice arranged in $1/8$ inch Si_3N_4 spheres.¹⁹ The Si_3N_4 has a fairly high dielectric constant $\epsilon = 8.67$ ($n = 2.95$) and a very small loss of $4.5 \times 10^{-3} \text{ mm}^{-1}$ of the electromagnetic (EM) field in the millimeter wavelength region. The Si_3N_4 balls are used for high-precision ball bearings and are therefore guaranteed to possess a perfect spherical shape and quite uniform size. Therefore it was expected that the experimental results were reproduced by theoretical calculations. In fact, a major part of the calculations is in agreement with the experimental results, but there are small differences between experimental results and calculations, for example, missing photonic bands in dispersion curves, the intensity of the transmittance in the high-frequency region, and the width of the structure in the spectra. These differences have been found in previous reports, which deals with the monolayer lattice using polyvinyltoluene (latex) spheres.^{17,18}

Furthermore, the optical properties of 3D photonic crys-

tals using dielectric spheres have been reported.^{20–23} In investigating these 3D photonic crystals, the most important problem is the distortion and imperfections in crystals, because it is difficult to control the sphere’s positions due to the visible wavelength region. Moreover, the effect of absorption and the size dispersion of the spheres may obscure the intrinsic properties. Therefore theoretical analysis was important to explain the observed phenomena. However, the experimental spectra have not been compared with theoretical calculations, and the effects of the photonic bands in the 3D photonic crystals have not been discussed in detail.

In this paper, the optical properties of the monolayer triangle lattice and 3D photonic crystals built by Si_3N_4 spheres have been investigated. To discuss the effect of the loss, the experimental results are compared with the theoretical spectra using the complex dielectric constant. In order to analyze the data of the monolayer lattice, the difference between the experimental dispersion curves and theoretical calculations is compared and the reasons of missing photonic bands are discussed. Moreover, the photonic band effects of the 3D photonic crystals are discussed. Finally, we discuss future prospects of photonic crystals using dielectric spheres.

II. EXPERIMENTAL SETUP

Spherical balls of Si_3N_4 (made by Toshiba Tungaloy Co., Ltd.) with diameter $d = 1/8$ in. (3.175 mm) were used for the building blocks for the monolayer photonic crystal. Figure 1(a) shows the photograph of the monolayer triangle lattice made by Si_3N_4 spheres. The lattice constant a_L is equal to the sphere diameter. And the 3D photonic crystal was fabricated by arranging the monolayer periodic array (triangle lattice) of Si_3N_4 beads. Figure 1(b) shows the illustration of the 3D photonic crystal for eight layers. The Si_3N_4 are fixed by the frame with thickness 3.175 mm. The air gaps are controlled by putting the plates with various thicknesses between frames. The thickness of the plate is varied between

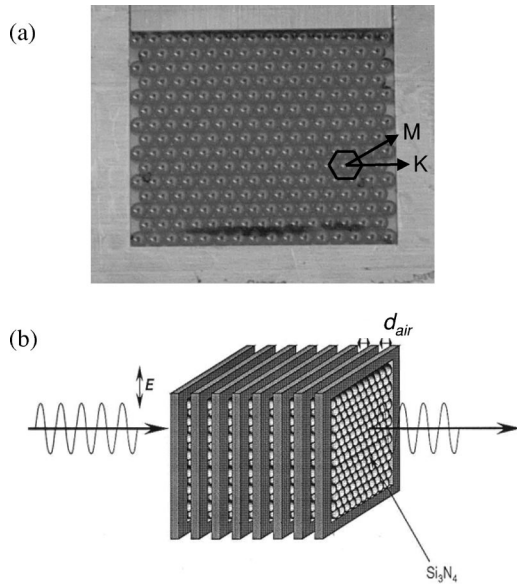


FIG. 1. (a) Photograph of the monolayer triangle lattice. The diameter of Si_3N_4 is 1/8 inch (3.175 mm). The dielectric constant is 8.67 and the loss is $4.5 \times 10^{-3} \text{ mm}^{-1}$. (b) The illustration of 3D photonic crystal of eight layers. The space between 2D lattices is divided by air.

0.3 and 3.1 mm, that is, the distance of the air gap (d_{air}), and represents the shortest distance between two monolayers. The Si_3N_4 balls in a plane lattice are located on the top of balls in the next lattice. Therefore the crystal structure is simple hexagonal (D_{6h}). And the lattice constant $a = b \neq c$.

The transmittance spectra of the monolayer lattice were measured by using a network analyzer (WILTRON 360B) as a function of the millimeter wave frequency for various angles of incidence of the EM wave. The experimental configuration of the measurement was shown in a previous paper.¹⁹ The frequency range is from 40 to 60 GHz. The frequency (ν) is normalized by $2c/\sqrt{3}a_L$. Here, a_L is the

lattice constant, i.e., the diameter of the Si_3N_4 sphere ($=3.175 \text{ mm}$). Therefore the observed frequency range corresponds to the normalized frequency range from 0.37 to 0.55. An incident wave then excites two kind of photonic band mode of the monolayer lattice whose \mathbf{k} vectors are on the symmetry axis Γ - K and Γ - M of the 2D Brillouin zone as shown in Fig. 1(a). Measurements were performed for S and P polarized EM waves for the Γ - K and Γ - M direction. The incident angle was varied from $\theta=0^\circ$ to 30° with a step width of 3° . The transmittance spectra of the 3D photonic crystals were also measured by same network analyzer for normal incidence. The polarization of the EM wave is parallel to the Γ - M direction for the monolayer lattice as shown in Fig. 1(b).

The experimental results are compared with theoretical calculations. Calculations were performed for $d = 3.175 \text{ mm}$ and $n = 2.95 + 0.01i$. In this calculation, a complex refractive index was used since the Si_3N_4 causes a loss (absorption) of the EM wave. The value of the imaginary part was estimated from the loss $4.5 \times 10^{-3} \text{ mm}^{-1}$. The detailed methods of the theoretical calculations were reported in a previous paper.¹⁹

III. RESULT AND DISCUSSION

A. Photonic band effect of monolayer triangle lattice

The transmittance spectra are shown in Fig. 2 for Γ - M (MP and MS) and Γ - K (KP and KS) directions. In Figs. 2(b) and (c), the interference was observed at the high-frequency region at small angles. Although it is difficult to distinguish the fine structure from the transmittance spectra in the high-frequency region, one can distinguish the broad humps from the spectra. Since the only broad humps were found in Figs. 2(a) and (d), the fine structures were not picked up in the high-frequency region in Figs. 2(b) and (c). Except the interference, remarkable dependence of angle was found in different polarizations and directions with increase of the incident angles.

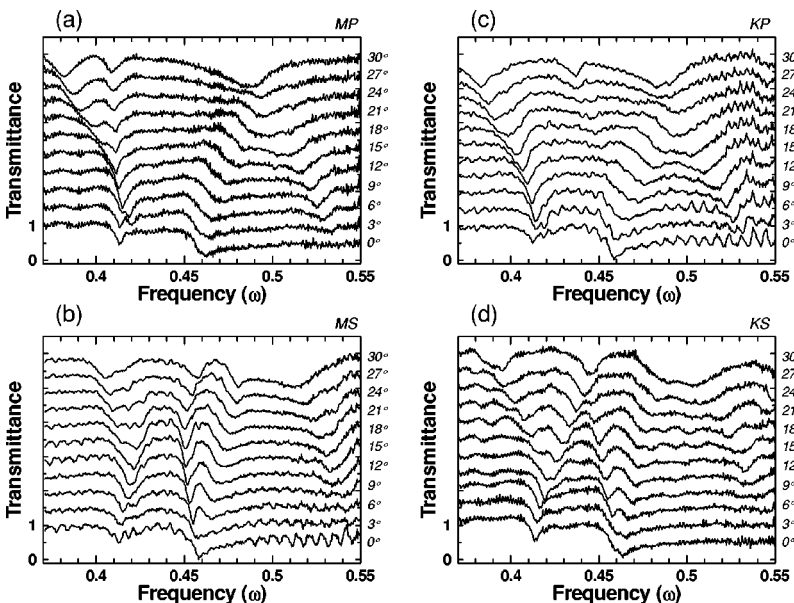


FIG. 2. Transmittance spectra of S and P polarized wave for the Γ - M and Γ - K direction vs various incident angles. (a) shows the spectra of P polarized wave for the Γ - M direction. (b) shows those of the S polarized wave for the Γ - M direction. (c) shows those of the P polarized wave for the Γ - K direction. (d) shows those of S polarized wave for the Γ - K direction. Horizontal axis shows the normalized frequency range 0.37–0.55.

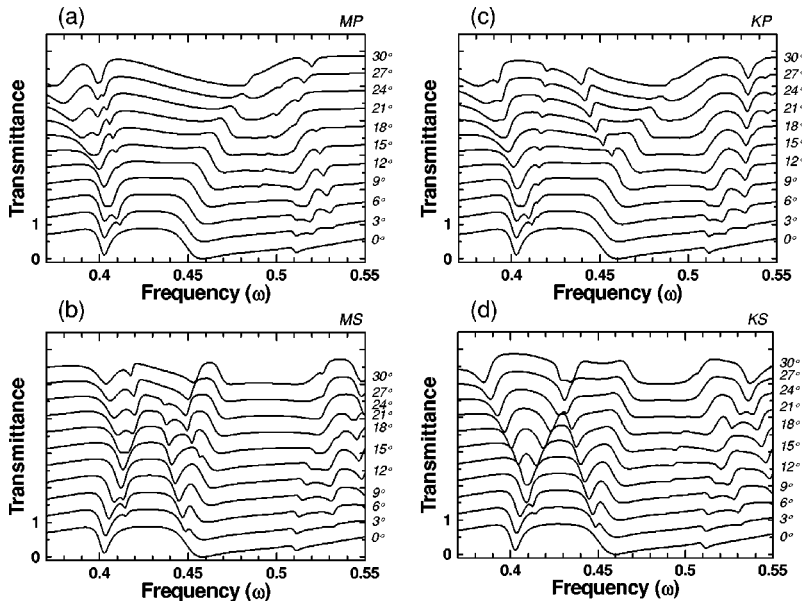


FIG. 3. Calculated transmittance spectra of S and P polarized wave for Γ - M and Γ - K direction vs various incident angles. (a)–(d) correspond to Figs. 2(a)–(d), respectively.

Here, the fine structures in transmittance spectra are examined. The two dips were found at 0.41 and 0.46 for $\theta = 0^\circ$ in each spectrum. And widths and frequencies of the dips were changed with increasing θ . Moreover, the new dips appeared for off-normal incident angles. Comparing with the spectra shown Figs. 2(a)–(d), it is concluded that the fine dips in the all spectra are quite independent of each other. This means that the photonic band structures of the monolayer lattice for two directions and two polarizations differ from each other. The calculation curves are shown in Figs. 3(a)–(d) for all directions and polarizations. The intensity and shape of the transmittance are well reproduced by the theoretical calculation. Because of the usage of the complex refractive index, this agreement is much better than that reported in our previous paper.¹⁹

From the frequency of observed dips and humps in all directions, the experimental dispersion relations (ω - k) are plotted in Figs. 4(a) and (b) using filled circles, open circles, and crosses, which stand for the deep, intermediate, and shallow dips, respectively. Upper and bottom figures show the P - and S -polarized wave, respectively. The photonic bands of Γ - K direction are shown on the right-hand side, and those of Γ - M are on the left-hand side. As compared with Figs. 4(a) and (b), it is found that the similarity between the photonic band structure of MP (KP) and MS (KP) at the Γ point is quickly lost as k increases. In Fig. 4(c) and (d), theoretical photonic band structures are shown by crosses and open squares as a function of wave vector k . Two kinds of marks indicate the parities of the photonic bands. However, it is too difficult to distinguish the parities from experimental results.

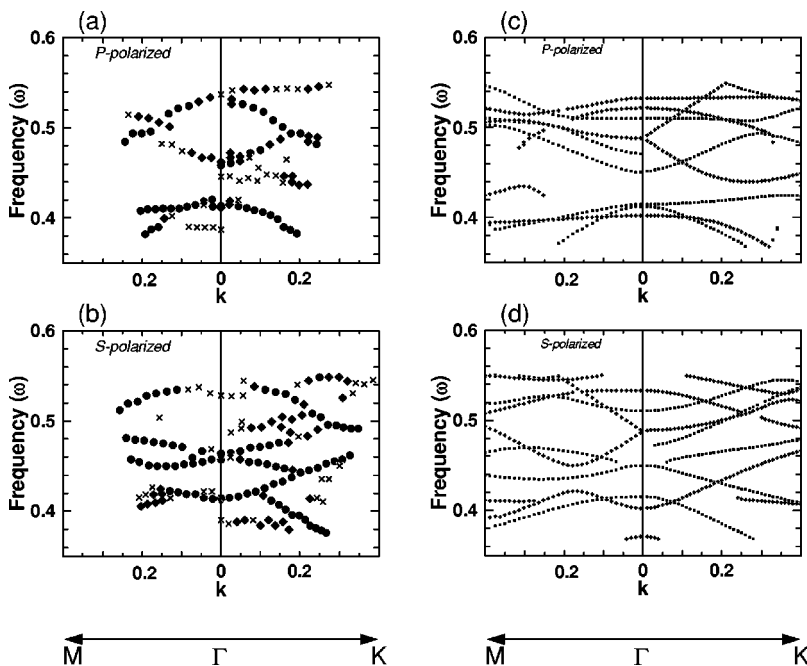


FIG. 4. ω - k relations of the monolayer triangle lattice. (a) and (b) represent the respective fine structures (dip positions) estimated by the experimental results. The filled circles, open circles, and crosses stand for the deep, intermediate, and shallow dips, respectively. (c) and (d) are calculations. Horizontal axis of the left-hand side represents the wave number of Γ - M , the right-hand side is the wave number of Γ - K . Vertical axis is normalized frequency.

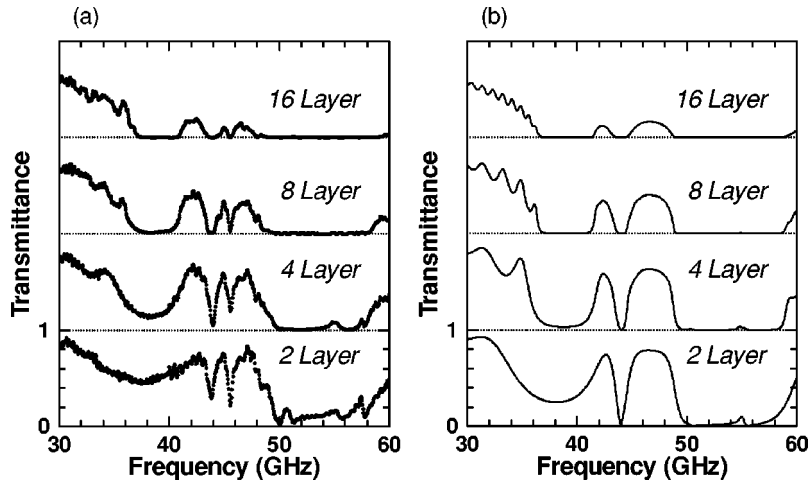


FIG. 5. The transmittance spectra of 3D photonic crystals made by layering the 2D triangle lattices. (a) shows the experimental result for 2–16 layers, and (b) shows theoretical calculations. The air gap is 0.3 mm. Horizontal axis shows the frequency range 30–60 GHz. The parameters of the calculation were $a_L = 3.175$ mm and $n = 2.95 + 0.01i$.

Comparing the experimental results and the calculation, it is seen that the photonic bands at about 0.41, 0.46, and 0.53 are in good agreement with the calculation. The agreement is remarkable if we consider the fact that we used only two material parameters of the diameter $d = a_L$ and the dielectric constant ϵ .

Nevertheless, some photonic bands are not observed in experiment and theoretical spectra. For example, photonic bands coming from 0.50 or upper frequency at the Γ point in Figs. 4(c) and (d) are not observed. The missing photonic bands have been explained by the inactivity of the mode of the photonic band for the polarity of the incoming EM wave.²⁴ In the current paper, we propose another reason based on the analysis of the theoretical transmittance spectra. As shown in Fig. 3, the sharp dips and peaks are not found in the theoretical transmittance spectra using the complex dielectric constant. However, if the loss of the EM wave is neglected in the calculated curves, several sharp dips or peaks appear at the high-frequency region, as reported in a previous paper.¹⁹ It is suggested that the photonic bands estimated by the sharp dips or peaks are obscured by the loss (absorption) of the EM wave. These phenomena are explained as follows: If there is a loss in the photonic crystal, the lifetime of the mode of the photonic band becomes longer. Due to the longer lifetime of the mode, broadening of the dips and peaks take place. Therefore the sharp dips and peaks are smoothed and merged by the absorption and some of photonic bands are difficult to observe in the transmittance spectra.

B. Transmittance spectra of 3D layered photonic crystals

Figure 5(a) shows the transmission spectra of different layered 3D photonic crystals for the distance of air gaps $d_{air} = 0.3$ mm. The incident EM waves were normal and the transmitted EM waves were detected in the range 26–60 GHz. It seems that the broad high reflective region is at 36–40 GHz. In this region, the edge is sharper and the transmittance is decreased to nearly zero with increase of the number of layers. The other high reflective region is found at 43 and 46 GHz. The widths of these regions are narrower than that at 36–40 GHz. The structures at high frequency

(>50 GHz) are not clear. From the shapes of all high reflective regions, it is found that four or eight times periodicity is enough to make photonic band gaps. In order to investigate the experimental results, the transmission spectra for the 3D photonic crystal were calculated using the same parameters $a_L = 3.175$ mm and $n = 2.95 + 0.01i$ as the monolayer lattice. The results are shown in Fig. 5(b). As compared with Fig. 5(a), the intensity and shape agree well with the experimental spectra. However, the dip near 46 GHz is not found in the calculation. It is considered that the dip was observed because of the distortion of the lattice or/and the off-normal incidence of the EM wave.

Next, the distance of air gap (d_{air}) was changed 0.3, 0.8, 1.0, 1.6, 2.0, 2.6, and 3.1 mm. The transmission spectra are shown in Fig. 6: (a) shows experimental results and (b) is theoretical calculations. The number of layers is 16. The high reflective region at 36–40 GHz for 0.3 mm is shifted to the low-frequency region (long-wavelength region) with increase of the distance of the air gap. And the width of the high reflective region became wider until $d_{air} = 1.6$ mm and beyond that number narrower. In contrast, the band gap near 43 GHz kept its frequency and width. Moreover, the other high reflective region is found at 47 GHz for $d_{air} = 1.6$ mm. This region is shifted to lower frequency with increase of the distance of air gaps. It is overlapped with the high reflective region at 43 GHz observed for $d_{air} = 0.3$ mm when the air gap is 2.6 mm. Furthermore, it is shifted to 42 GHz when d_{air} is 3.1 mm. This shift is similar to the high reflective region observed at 36–40 GHz for 0.3 mm.

In Figs. 5(a) and 6(a), the transmittance in the higher frequency region is almost zero and the fine structure is not observed clearly. In this paper, only a small imaginary part of the refractive index was assumed; the intensity and the shape of the observed transmittance spectra agree very well with the calculation. The decrease of the transmittance intensity in high frequency was also observed for the monolayer lattice.¹⁷ These phenomena are explained by the loss of the EM wave. As mentioned above, the lifetime of the mode of the photonic band becomes longer by absorption. In general, the mode lifetime with larger angular momentum l becomes longer than that with smaller one. Additionally, the density of

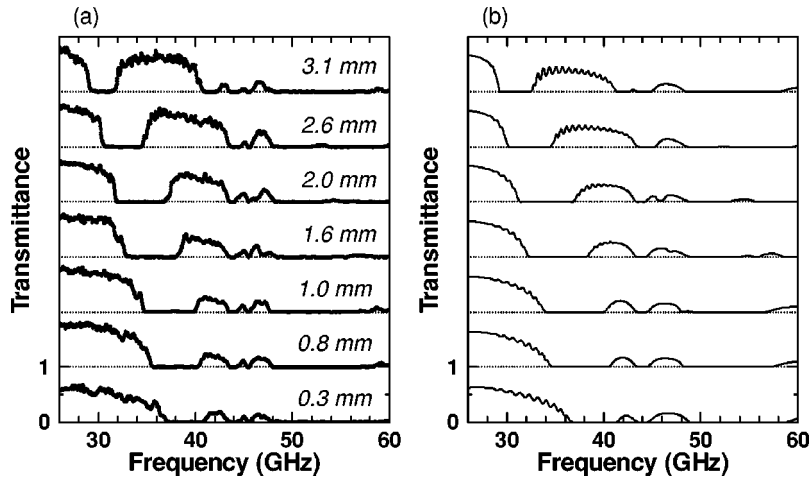


FIG. 6. Transmission spectra of the different air gap d for a 16-layer crystal. The spectra are shown for $d_{air}=0.3\text{--}3.1$ mm. (a) and (b) show the experimental data and theoretical calculations, respectively. The parameters of the calculation were $a_L=3.175$ mm and $n=2.95+0.01i$.

modes in the high-frequency region is larger than that in the low-frequency region. From these effects therefore the transmitted EM wave in the high-frequency region is weaker than that in the low-frequency region and its intensity rapidly decreases with increase of the thickness (number of layers) like the spectra shown in Fig. 5.

C. Origin of the photonic band gaps for 3D photonic crystals

Here, we discuss the origin of the high reflective regions observed in transmittance spectra. In order to investigate the relation of the high reflective region and the photonic band gap, the transmittance spectra were compared with theoretical photonic band structures. Figure 7 shows photonic band structures and experimental and calculated transmittance spectra. From this figure, the observed high reflective regions show good agreement with the band gap. This means that the observed high reflective regions are considered as the photonic band gaps. In the observed photonic band gaps, as shown in Fig. 6, the photonic band gap at 36–40 GHz for $d_{air}=0.3$ mm changes its frequency and width with increase of the space of air gaps. On the other hand, the photonic band gap at 43 GHz does not change its frequency and width. The shift of band gap is explained as follows. If the distance of the air gap becomes wider, the Brillouin zone is smaller. Then, the turning wave number of the Brillouin zone is changed to lower frequency, and the frequency at the edge of the Brillouin zone as decreasing. Therefore the band gaps are changed in the lower energy range with increasing of the distance of the air gap. In contrast, as compared with transmittance spectra shown in Fig. 2 ($\theta=0^\circ$), it is expected that the band gap as related to the photonic band effect of the monolayer lattice since the fine dip was also observed at the same frequency for the monolayer triangle lattice. In fact, one can see that two photonic bands are anticrossing near 44 GHz in both band structures for 0.3 mm, and that for 3.1 mm, as shown in Fig. 7. In other words, the band of light photons and that of heavy photons are interacting and anticrossing near 44 GHz. As a result, the photonic band gap opens near 43 GHz and does not change its frequency and width.

Moreover, the width of the band gap is discussed. As mentioned above, the width of the stop band becomes wide

until $d_{air}=1.6$ mm, and after then it becomes narrow. In general, it is expected that the width of the first band gap becomes narrower with increase of the distance of air gap, because the average dielectric constant is close to unity. In contrast, the change of the width of the higher-ordered band gap is complicated because the amount of shift at the upper

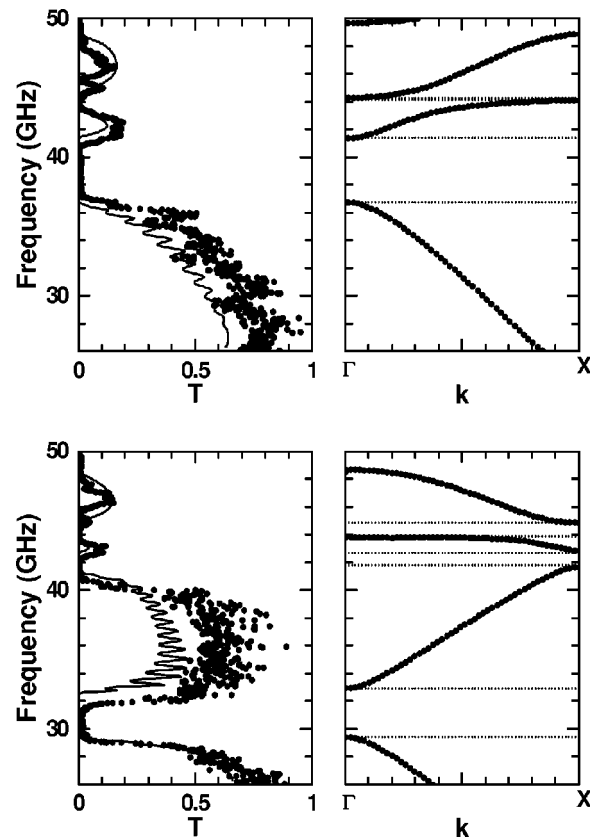


FIG. 7. Photonic band structures and experimental and calculated transmittance spectra. The upper and lower spectra have been measured with an air gap of 0.3 and 3.1 mm, respectively. The figures on the left-hand side show the transmittance spectra. The solid lines are theoretical calculations and the large circles are the experimental results. The figures on the right-hand side show the photonic band structure in the direction normal to the lattice plane. The band structure is calculated for infinite periodicity.

photonic band is different from that at the lower band. This behavior is similar to that of 2D photonic crystals. In general, the band gaps were calculated by changing the filling factor and showed that the width of the band gap depended on the filling factor. Here, if the filling factor corresponds to the distance of air gap in our experiment, the change of the band gap is understood.

D. Future prospect of photonic crystals using dielectric spheres

Finally, we consider the future prospect of the photonic crystals using dielectric spheres. Recently, photonic crystals with full band gaps were fabricated using a GaAs wood pile structure by Noda *et al.*^{25,26} This crystal has a full band gap in the infrared region, and beyond the analysis of optical properties, applications for optoelectric devices are expected. Furthermore, an interesting method that is called the auto-cloning technique was used to produce 3D photonic crystals.^{27,28} Although these crystals do not have a full band gap, they are used to study the optical properties for devices because of good periodicity and the photonic bands in the infrared to visible spectral region. Thus photonic crystals whose unit size is submicrometer are fabricated by different techniques. These crystals have a good periodicity and the photonic bands are located in the visible wavelength region. With this material, interesting optical phenomena like a superprism effect were observed.²⁹ Therefore it is expected that these crystals will form optical devices, since one can fabricate the suitable photonic crystals for application by controlling the structure. However, the structure of these crystals is complicated and theoretical analysis of the observed phenomena is not so easy. On the other hand, in the crystals using dielectric spheres, although the photonic band gaps are controlled by changing the distance of the air gap as shown in Fig. 6, it is difficult to arrange the submicrometer-sized

spheres. From this viewpoint, photonic crystals using dielectric spheres are not expected to deliver useful hosts for optical applications, but considering the good agreement between the experimental results and the theoretical calculations, the system of arranged dielectric spheres is useful for analysis of the physical properties.

IV. SUMMARY

A monolayer triangle lattice was fabricated by millimeter-sized Si_3N_4 spheres. The transmittance spectra were measured for different angles in the normalized frequency range 0.37–0.55 and many dips in the transmittance were observed and calculated using the diameter and the complex dielectric constant of Si_3N_4 . Independent of photonic band effects the observed dips exhibit an angle dependence for all spectra. As a result of the comparison with the dispersion relation of the photonic bands in the infinite triangle lattice, it is considered that several photonic bands are merged due to the absorption of dielectric spheres. Furthermore, 3D layered photonic crystals were fabricated and their transmittance spectra were measured for different layers and different air gaps by normal incidence of the EM wave. From these spectra, the formation of the photonic band gaps was observed and the effect of the loss (absorption) was discussed. The photonic band gaps referred to the anticrossing between heavy photon band and light photon band. Finally, we discussed the future prospect of the photonic crystals using dielectric spheres.

ACKNOWLEDGMENTS

This work was partially supported by Special Coordination Funds and Grants-Aid for Scientific Research from the Ministry of Education, Culture, Sports, Science and Technology of the Japanese Government.

*Present address: Department of Physics and Astronomy, Bowling Green State University, OH 43403.

¹E. Yablonovitch, Phys. Rev. Lett. **58**, 2059 (1987).

²E. Yablonovitch, J. Phys.: Condens. Matter **5**, 2443 (1993).

³J. Opt. Soc. Am. B **10**, 1 (1993) (Special issue on photonic crystals).

⁴K. Ohtaka, Phys. Rev. B **19**, 5057 (1979).

⁵N. Stefanou, V. Karathanos, and A. Modinos, J. Phys.: Condens. Matter **4**, 7389 (1992).

⁶X. Wang, X.-G. Zhang, Q. Yu, and B.N. Harmon, Phys. Rev. B **47**, 4161 (1993).

⁷T. Suzuki and P.K.L. Yu, J. Opt. Soc. Am. B **12**, 570 (1995).

⁸K. Ohtaka and Y. Tanabe, J. Phys. Soc. Jpn. **65**, 2265 (1996).

⁹K. Ohtaka and Y. Tanabe, J. Phys. Soc. Jpn. **65**, 2670 (1996).

¹⁰K. Ohtaka and Y. Tanabe, J. Phys. Soc. Jpn. **65**, 2270 (1996).

¹¹K. Ohtaka, T. Ueta, and Y. Tanabe, J. Phys. Soc. Jpn. **65**, 3068 (1996).

¹²K. Ohtaka, H. Miyazaki, and T. Ueta, Mater. Sci. Eng., B **48**, 153 (1997).

¹³E.R. Brown and O.B. McMahon, Appl. Phys. Lett. **67**, 2138 (1995).

¹⁴I.I. Tarhan, M.T. Zinkin, and J.H. Watson, Opt. Lett. **20**, 1571 (1995); Phys. Lett. B **68**, 3506 (1996).

¹⁵I.I. Tarhan and G.H. Watson, Phys. Rev. Lett. **76**, 315 (1996).

¹⁶T. Fujimura, K. Edamatsu, T. Itoh, R. Shimada, A. Imada, T. Koda, N. Chiba, H. Muramatsu, and T. Ataka, Opt. Lett. **22**, 489 (1997).

¹⁷H.T. Miyazaki, H. Miyazaki, K. Ohtaka, and T. Sato, J. Appl. Phys. **87**, 7152 (2000).

¹⁸R. Shimada, Y. Komori, T. Koda, T. Fujimura, T. Itoh, and K. Ohtaka, Mol. Cryst. Liq. Cryst. Sci. Technol., Sect. A **349**, 5 (2000).

¹⁹K. Ohtaka, Y. Suda, S. Nagano, T. Ueta, A. Imada, T. Koda, J.S. Bae, K. Mizuno, S. Yano, and Y. Segawa, Phys. Rev. B **61**, 5267 (2000).

²⁰H. Miguez, C. Lopez, F. Meseguer, A. Blanco, L. Vazquez, R. Mayoral, M. Ocana, V. Fornes, and A. Mifsud, Appl. Phys. Lett. **71**, 1148 (1997).

²¹E.P. Petrov, V.N. Bogomolov, I.I. Kalosha, and S.V. Gaponenko, Phys. Rev. Lett. **81**, 77 (1998).

²²G. Subramania, K. Constant, R. Biswas, M.M. Sigalas, and K.M. Ho, Appl. Phys. Lett. **74**, 3933 (1999).

- ²³R.M. Amos, J.G. Rarity, P.R. Tapster, T.J. Shepherd, and S.C. Kitson, *Phys. Rev. E* **61**, 2929 (2000).
- ²⁴W.M. Robertson, G. Arjavalingam, R.D. Meade, K.D. Brommer, A.M. Rappe, and J.D. Joannopoulos, *Phys. Rev. Lett.* **68**, 2023 (1992).
- ²⁵S. Noda, N. Yamamoto, H. Kobayashi, M. Okano, and K. Tomoda, *Appl. Phys. Lett.* **75**, 905 (1999).
- ²⁶S. Noda, K. Tomoda, N. Yamamoto, and A. Chutinan, *Science* **289**, 604 (2000).
- ²⁷S. Kawakami, *Electron. Lett.* **33**, 1260 (1997).
- ²⁸T. Kawashima, K. Miura, T. Sato, and S. Kawakami, *Appl. Phys. Lett.* **77**, 2613 (2000).
- ²⁹H. Kosaka, T. Kawashima, A. Tomita, M. Notomi, T. Tamamura, T. Sato, and S. Kawakami, *Phys. Rev. B* **58**, R10 096 (1998).